Agricultural and Forest Meteorology 218–219 (2016) 65–73

Contents lists available at ScienceDirect

Agricultural and Forest Meteorology

journal homepage: www.elsevier.com/locate/agrformet

Process-based rainfall interception by small trees in Northern China: The effect of rainfall traits and crown structure characteristics

Xiang Li[a], Qingfu Xiao[b], Jianzhi Niu[a,*], Salli Dymond[c], Natalie S. van Doorn[d], Xinxiao Yu[a], Baoyuan Xie[a], Xizhi Lv[e], Kebin Zhang[a], Jiao Li[a]

[a] Key Laboratory of Soil and Water Conservation and Desertification Combating of Education Ministry, Beijing Forestry University, Beijing 100083, China
[b] Department of Land, Air and Water Resources, University of California, Davis, CA 95616, USA
[c] USDA Forest Service, Pacific Southwest Research Station, Davis, CA 95618, USA
[d] USDA Forest Service, Pacific Southwest Research Station, Albany, CA 94710, USA
[e] Yellow River Institute of Hydraulic Research, Key Laboratory of the Loess Plateau Soil Erosion and Water Loss Process and Control of Ministry of Water Resources, Zhengzhou 450003, Henan, China

ARTICLE INFO

Article history:
Received 19 June 2015
Received in revised form 6 November 2015
Accepted 23 November 2015
Available online 17 December 2015

Keywords:
Rainfall interception storage
Post-rainfall drainage
Rainfall intensity
Leaf area
Branch density

ABSTRACT

Rainfall interception by a tree's crown is one of the most important hydrological processes in an ecosystem, yet the mechanisms of interception are not well understood. A process-based experiment was conducted under five simulated rainfall intensities (from 10 to 150 mm h^{-1}) to directly quantify tree crown interception and examine the effect of rainfall traits and crown structure characteristics on interception for broadleaf (*Platycladus orientalis*, *Pinus tabulaeformis*) and needle tree species (*Quercus variabilis*, *Acer truncatum*). Results indicated that (1) the interception process was composed of three phases, a rapid increase phase which accounted for approximately 90% of the maximum interception storage (C_{max}), a relatively-stable phase, and a post-rainfall drainage phase in which 40% (±16%) of C_{max} drained off to reach the minimum interception storage (C_{min}); (2) C_{max} and C_{min} were only correlated with rainfall intensity for *P. tabulaeformis*; (3) C_{max} and C_{min} were correlated with both leaf traits (i.e., leaf area, leaf biomass, leaf morphology) and branch traits (i.e., branch density, branch count, branch length, woody surface area, and woody biomass), and the best predictors of C_{max} and C_{min} were biomass-related parameters; and (4) The needle species *P. orientalis* had the greatest C_{max}, while the largest C_{min} was observed in the broadleaf species *A. truncatum*. Our findings demonstrate the complexity of the interception process and tree characteristics may be more important in controlling interception than rainfall characteristics.

1. Introduction

In forest, rainfall is either intercepted by a tree's crown (i.e. leaves and branches) or falls down to the ground (Xiao and McPherson, 2015). Rainfall interception can account for 10-50% of gross precipitation (Llorens and Domingo, 2007; Carlyle-Moses and Gash, 2011), and has various hydrological and ecological functions. For instance, it smoothes rainfall, thereby enabling more gradual infiltration (Gerrits et al., 2010), while reducing floods and soil erosion (Xiao et al., 2000a; Xiao and McPherson, 2003; Morgan, 2005). More broadly, interception greatly impacts the energy balance (van Dijk et al., 2015), chemical deposition (Xiao and McPherson, 2011), insecticides, fungicides and fertilizer efficiency (Aston, 1979), total evaporation (Savenije, 2004), water availability for plant growth and biomass (Sutanto et al., 2012), and global water resources (Murray, 2014).

In general, there are two types of interception storage (Li et al., 2013). The maximum interception storage (C_{max}) is the amount of rainwater intercepted and stored by the tree crown immediately before rainfall cessation. The minimum interception storage (C_{min}) is the amount of rainwater detained on the crown when surface drainage ceases after rainfall; C_{min} can only be removed by evaporation. C_{min} values have been widely reported in previous studies given that it is equal to the evaporative loss and can be easily measured by the difference between gross rainfall and net rainfall (thoughfall + stemflow) (van Dijk et al., 2015). Throughfall has been primarily collected by only a few gauges which were randomly positioned beneath the crown. However, hundreds even thousands of gauges are required to capture the spatial variability in throughfall (Kimmins, 1973) – the throughfall distribution

* Corresponding author. Tel.: +86 10 62336009.
E-mail address: nexk@bjfu.edu.cn (J. Niu).

http://dx.doi.org/10.1016/j.agrformet.2015.11.017
0168-1923/

was uneven and was correlated with distance from the tree trunk (Nanko et al., 2011; Fathizadeh et al., 2014). Not accounting for this and thus may introduce errors in C_{min} as high as 30% (Muzylo et al., 2009).

In comparison, C_{max} has been largely disregarded in previous studies mainly due to difficulty in measurements. Nevertheless, the difference between C_{max} and C_{min} represents the post-rainfall drainage, along with drainage duration, which reveals how the rainfall-lagging effect is exerted via interception (Guevara-Escobar et al., 2007).

Rainfall interception studies indicate that interception is controlled by three groups of variables (Xiao et al., 2000b; Gerrits and Savenije, 2011): (1) rainfall characteristics such as rainfall intensity and gross precipitation; (2) crown structure characteristics, like leaf area index and leaf morphology; and (3) meteorological parameters such as wind speed, relative humidity, and net radiation. However, there is conflicting information regarding to process by which interception interacts with these variables. For example, no consensus has been reached on the effect of rainfall intensity on interception. Some studies suggest that interception increases with increasing rainfall intensity because of gradual saturation of the crown (e.g. Aston, 1979; Keim et al., 2006), while other studies show that higher rainfall intensities result in lower interception because raindrops cannot be stored on leaves and branches while the crown is agitated by intense rainfall (e.g. Horton, 1919; Wang et al., 2007). In addition, previous interception studies involve large forest stands and individual mature trees, where many structure characteristics cannot be easily measured (e.g. leaf area, leaf biomass, branch inclination, branch density etc.) (Levia et al., 2015). As a result, the relationship between interception and crown characteristics remains unclear (Nanko et al., 2013).

Hence, a process-based experiment is needed to accurately measure interception, and to further investigate the mechanisms of interception processes. This is especially important in Northern China, where water scarcity and soil erosion have become increasing threats to sustainable development (Ministry of Water Resources of P. R. China, 2011, 2013; Wang et al., 2015), and where large-scale re-forestation efforts are altering rainfall distribution and regional water budgets (Chen et al., 2005; Wang et al., 2011).

The main objectives of this study are to: (1) directly quantify C_{max} and C_{min} on a process basis; (2) elucidate the impact of rainfall characteristics (e.g. rainfall intensity and gross precipitation) on interception; and (3) study the relationship of C_{max} and C_{min} with structure characteristics.

2. Materials and methods

2.1. Tree species

Four dominant tree species in the Northern China forest were selected for this study. Four trees were selected for each tree species. The experimental trees were selected from Jiufeng National Forestry Park, Beijing, China (116°28′E, 39°34′N), and were transported to the rainfall simulation laboratory (Key Laboratory of Soil and Water Conservation of Chinese Education Ministry in Beijing, China). These sample trees were approximately five-year old. Coniferous species were represented by *Platycladus orientalis* (*PO*) and *Pinus tabulaeformis* (*PT*); and broadleaf trees were represented by *Quercus variabilis* (*QV*) and *Acer truncatum* (*AT*). Upon arriving in the laboratory, each tree was re-planted in individual 2-m-diameter plastic cylinder with native soil. Tree structure characteristics were measured prior to the rainfall experiments (Table 1). Leaf area index (LAI), which is defined as total leaf area divided by crown projection area, was measured by the LAI-2200 Plant Canopy Analyzer device (LICOR Inc., Lincoln, NE, USA). More details about the device were given by Kobayashi et al. (2013). In our study, two LAI readings were collected both above and below the crown in each cardinal direction; these 16 measurements were then averaged to determine tree LAI. The crown projected area was determined using photograph analysis method. Pictures were taken at a height of 15 m above the tree crown, and were further analyzed in Adobe Photoshop. As there were very few secondary branches, only the mean primary branch angle was measured using a protractor. Other

Table 1
Characteristics of the experimental trees.

Tree species	H (m)	CH (m)	D_B (cm)	LAI	CPA (m^2)	TLA (m^2)	WSA (m^2)	TSA (m^2)	MPBA (°), (STD)	LB (kg)	WB (kg)	TB (kg)	TLC (*n*)	TBC (*n*)	TBL (m)	LD_{min} ($n\,m^{-3}$)	BD_{min} ($n\,m^{-3}$)
PO-1	1.7	1.5	1.6	2.84	0.91	2.58	0.21	2.79	63.9 (10.3)	0.53	0.69	1.22	44942	201	47.2	39294	147
PO-2	1.8	1.6	1.6	2.68	1.20	3.22	0.31	3.53	55.4 (8.8)	0.76	0.73	1.49	51775	255	45.5	26966	133
PO-3	2.3	1.9	2.1	1.60	1.12	1.79	0.34	2.13	69.6 (11.6)	0.50	0.51	1.01	35457	244	34.2	16662	115
PO-4	2.7	2.1	2.3	2.18	0.81	1.77	0.44	2.21	82.2 (14.1)	0.49	0.63	1.12	31331	338	45.5	18419	114
Mean (PO)	2.1	1.8	1.9	2.33	1.01	2.34	0.33	2.67	67.8 (13.3)	0.57	0.64	1.21	40876	260	43.1	23742	127
PT-1	1.5	1.3	2.7	3.84	1.40	5.38	0.74	6.12	95.5 (5.5)	0.42	0.89	1.31	21337	95	25.5	11724	52
PT-2	1.2	1.0	2.1	3.51	1.30	4.56	0.43	4.99	88.3 (7.8)	0.35	0.86	1.21	15565	88	15.8	11973	68
PT-3	1.8	1.5	3.5	2.96	2.10	6.22	0.66	6.88	92.3 (4.2)	0.93	1.22	2.15	27352	118	31.2	8683	37
PT-4	1.9	1.7	4.1	2.99	1.75	5.23	0.57	5.80	87 (9.6)	0.83	1.09	1.92	19881	133	29.5	6682	45
Mean (PT)	1.6	1.4	3.1	3.33	1.64	5.35	0.60	5.95	90.7 (8.2)	0.63	1.02	1.65	21034	109	25.5	9766	51
QV-1	1.2	1.0	1.1	2.14	0.58	1.24	0.1	1.34	79.5 (8.5)	0.06	0.31	0.37	328	25	4.4	565	43
QV -2	3.0	2.7	1.9	2.77	0.82	2.27	0.28	2.55	71.7 (12.2)	0.11	0.49	0.60	868	37	6.8	392	17
QV -3	3.3	2.9	3.1	1.37	1.26	1.72	0.15	1.87	61.7 (11.5)	0.15	0.45	0.60	456	44	7.5	125	12
QV -4	3.7	3.3	4.2	0.96	1.94	1.86	0.24	2.10	74.5 (15.2)	0.18	0.48	0.66	647	62	12.3	101	10
Mean (QV)	2.8	2.5	2.6	1.81	1.15	1.77	0.19	1.96	71.9 (10.8)	0.13	0.43	0.56	575	42	7.8	296	20
AT-1	2.7	2.3	2.7	1.63	1.77	2.89	0.71	3.60	75.5 (13.5)	0.26	2.71	2.97	1232	456	50.9	303	112
AT -2	2.6	2.1	2.5	1.43	1.78	2.55	0.61	3.16	65.8 (10.2)	0.15	1.41	1.56	1009	408	55.3	270	109
AT -3	2.5	1.9	4.4	1.56	2.04	3.18	0.77	3.95	78.1 (14.2)	0.21	1.75	1.96	1066	441	65.5	275	114
AT -4	3.5	3.1	4.0	1.24	5.79	7.18	1.03	8.21	71.1 (16.7)	0.31	1.84	2.17	2555	548	82.1	142	31
Mean (AT)	2.8	2.4	3.4	1.47	2.85	3.95	0.78	4.73	72.6 (9.7)	0.23	1.93	2.17	1467	463	63.5	247	91

Note: PO = *Platycladus orientalis*; PT = *Pinus tabulaeformis*; QV = *Quercus variabilis*; AT = *Acer truncatum*; H = height; CH = crown height; D_B = basal diameter; LAI = leaf area index; CPA = crown projected area; TLA = total leaf area; WSA = woody surface area (including branch and stem); TSA = total surface area; PMBA = primary mean branch angle (measured above vertical level, where 90° indicates a horizontal branch); LB = leaf biomass; WB = woody biomass (including branch and stem); TB = total biomass; TLC = total leaf count; TBC = total branch count; TBL = total branch length; LD_{min} = minimum leaf density; BD_{min} = minimum branch density; STD = standard deviation.

structure parameters such woody area (WA) and woody biomass (WB) were measured after the end of all the simulations. No wilting phenomenon was observed before or during the experimental procedures.

2.2. Rainfall simulation system

We used a rainfall simulation system (QYJY-503 C, Qingyuan Measurement Technology, Co. Ltd, Xi'an, China) equipped with 200 nozzles. The system is able to simulate a wide range of rainfall intensities (10 to 300 mm h^{-1}) using various water pressure and nozzle sizes controlled by a computer system. The rainfall simulator was positioned 18 m above the tree crown to allow raindrops to reach terminal velocity and a rainfall uniformity of greater than 80% (Huo et al., 2015). The median diameter of the simulated raindrops ranged from 0.2 to 5.0 mm, which is similar to natural raindrop distribution and size (Huo et al., 2015). Based on a 50-year historical precipitation data in Beijing (Zhong et al., 2013), rainfall at intensities of 10, 20, 50, 100, 150 mm h^{-1} were chosen to represent regional rainfall conditions. Each tree was subject to each rainfall intensity for a period of 1 h and the rainfall simulation equipment was re-calibrated prior to each replication.

2.3. Experiment design

Each tree was positioned on an electronic weighing balance (EP-500, E&C Co. Ltd, Shanghai, China; minimum graduation: 0.1 g) and two aluminum covers positioned at a 30° angle were fashioned around the tree bole to prevent throughfall and stemflow from entering the soil (Fig. 1). The cover edges were located on the ground. The covers were neither physical contacted to the balance nor to the tree. In addition, the tree bole was surrounded by a plastic reverse-funnel so that any stemflow was collected and transported to the ground without entering the soil. The interception amount for each experimental tree during the rainfall simulations was calculated as the change in tree weight.

After rainfall began, tree weight was recorded at a 10-s-interval for the first minute, a 30-s-interval for the next 9 min, and a 1-min-interval for the remaining 50 min. C_{max} was calculated as the difference in tree weight before and after the simulation. Post-simulation, tree weight was recorded every 10 s for the first minute, every 30 s for the next 9 min and every minute until a weight change of <0.1 g was obtained. C_{min} was calculated as the difference in tree weight before the rainfall simulation and after the drainage ended. During the rainfall simulation period, water was poured onto the floor of the laboratory every minute to keep the air humidity relatively stable. Thus, evaporation of canopy surface water due to wind and solar radiation were neglectable in this indoor experiment. Every test was replicated once, resulting in a total of 160 simulations performed between May and August, 2014, with a mean air temperature of 24.5 °C in the lab.

Upon completing all of the rainfall simulations, the retaining water on the tree was shaken off manually. After being air-dried in the open air for 24 h, each tree was carefully divided into three sections: foliage, branch and above-ground trunk. Total leaf and branch count were collected for all of the trees. Total leaf area for each tree was determined according to leaf morphology. For broadleaf species, each leaf was outlined on paper and scanned electronically, and the area was calculated using Adobe Photoshop. For needle species, 20 needles were randomly selected from each primary branch, and their length and width were measured using a measuring tape (minimum graduation: 0.1 cm). The average length ($\bar{l}$) and width ($\bar{d}$) of needles in each primary branch were then determined. *P. tabulaeformis* needle geometry was regarded as a three-dimensional cone and the total leaf area (TLA_{PT}) was

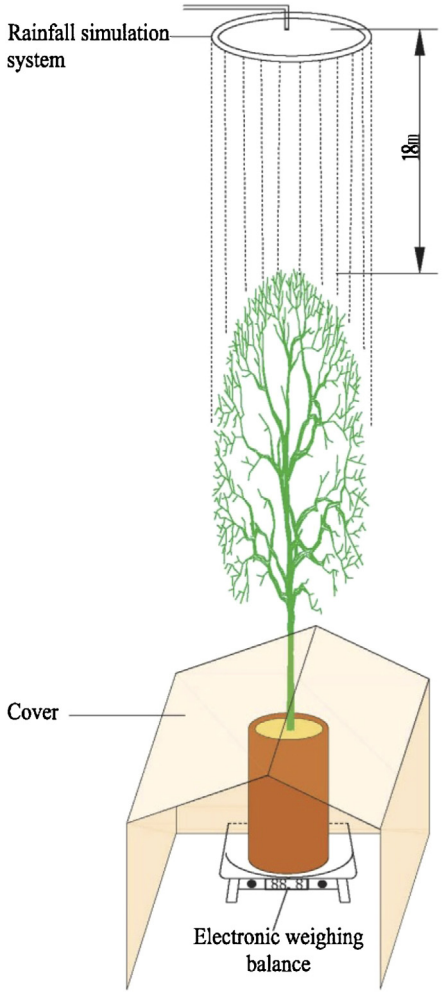

Fig. 1. Schematic of the rainfall interception experiment.

calculated by the combined areas of three triangles (Diao et al., 2010):

$$TLA_{PT}\left(m^2\right) = \sum_{i=1}^{m} \frac{3}{2} \overline{l_i} \overline{d_i}$$

where m is the total branch count for the tree, and $\overline{l_i}$ and $\overline{d_i}$ are the average length and width of branch i. Similarly, based on the column-geometry, the total leaf area of *P. orientalis* (TLA_{PO}) was calculated as:

$$TLA_{PO}\left(m^2\right) = \sum_{i=1}^{m} \pi \overline{d_i} \left(\frac{\overline{d_i}}{2} + \overline{l_i}\right)$$

where m is the total branch count for the tree, and $\overline{l_i}$ and $\overline{d_i}$ are the average length and width of branch i. The total leaf area (TLA) for the four species was recalibrated from LAI and CPA using the following equation:

$$TLA\left(m^2\right) = LAI \times CPA$$

Branch surface area was measured by cutting branches into several straight segments to measure lengths and diameters, which were then used to estimate the area as a column or three-dimensional cone. Trunk surface area was calculated as the trunk circumference multiplied by trunk length (length from the tree base to the first divergent branch). Woody surface area was then calculated by adding the branch and trunk surface areas from each tree.

Total branch length was measured and recorded as well (Table 1). In order to evaluate the leaf and branch distribution inside the crown, the minimum leaf density (LD_{min}) and branch density (BD_{min}) were determined by the following equations,

$$LD_{min}\left(nm^{-3}\right) = \frac{TLC}{CV_{max}} = \frac{TLC}{CH \times CPA}$$

$$BD_{min}\left(nm^{-3}\right) = \frac{TBC}{CV_{max}} = \frac{TBC}{CH \times CPA}$$

where TLC represents the total leaf count, TBC represents the total branch count, CH represents the crown height, CV_{max} represents the maximum crown volume, was calculated by CH multiplied CPA. The leaves and branches for each tree were oven-dried at 80 °C for 10 h, and leaf biomass and woody biomass were recorded as the dry weight (M_D) of each component. The total biomass was estimated by adding together leaf and woody biomasses. To further investigate the role of branch traits on interception, the mean distance between two leaves ($\overline{D_l}$) on each branch was calculated as follows:

$$\overline{D_l}(cm) = \frac{MBL}{MLC - 1} \times 100 = \frac{TBL/TBC}{TLC/TBC - 1} \times 100$$

where MBL is the mean length per branch, MLC is the mean leaf count per branch, TBL is the total branch length.

The maximum water storage capacity (S) of each tree was determined by completely immersing the branches, foliage, and trunks in water. In order to avoid the inner part of the branches and stems absorbing water and introducing error, their xylems were sealed with sealants. Subsequently, these samples were carefully transferred onto sample trays and soaked in water for 24 h achieve full saturation. Afterwards, they were taken out of the water and hung in the air for 20–30 min so that the drops on the surface of each section could drip off. The saturated weight (M_S) was measured after dripping ceased, and S was calculated as the difference between M_D and M_S.

2.4. Statistical analysis

Pearson's correlation coefficient was used to analyze the effect of rainfall characteristics (e.g. rainfall intensity and gross precipitation) and crown structure parameters (e.g. LAI, LA, WA, TB) on C_{max} and C_{min}, and linear, polynomial and non-linear regressions were used to determine the trend. Parameters were considered to be significantly correlated at or above the 95% confidence level ($p \leq 0.05$). One-way analysis of variance (ANOVA) and the Fisher LSD (Least Significant Difference) test ($p \leq 0.05$) was used to determine if there were significant differences in C_{max}, C_{min} and S among tree species. All statistical analyses were performed using IBM SPSS Statistics software (Ver. 20.0).

3. Results and discussion

3.1. Effect of rainfall characteristics on rainfall interception

Generally, cumulative interception storage increased rapidly at the beginning of the simulated rainfall because of the relatively dry crowns (Fig. 2). In the first minute, an average of 51.2% (±22.8%) of rainfall was intercepted across all species and rainfall intensities. The percentage of rainfall intercepted by the trees dropped dramatically to 9.2% (±5.9%) at the 10th minute, likely because the leaves and branches were largely saturated by the continuous rainfall. Meanwhile, C_{max} was achieved faster as rainfall intensity increased. In the first minute, cumulative interception storage accounted for 30.6% (±11.8%) of corresponding C_{max} at a rainfall intensity of 10 mm h^{-1}, compared with 91.4% (±13.5%) at 150 mm h^{-1}.

After approximately 10 to 15 min, the cumulative interception storage became relatively constant until the end of rainfall since the crown was gradually saturated and was unable to intercept additional water. Overall, C_{max} ranged from 0.30 (±0.10) to 0.88 (±0.14) mm across species with an average of 0.66 mm or 2.3% (±2.1%) of gross precipitation (Table 2). After rainfall cessation, 17%, 28% and 33% of C_{max} drained within the first 1, 5 and 10 min regardless of species. The drainage completely ceased after an average of 23 min

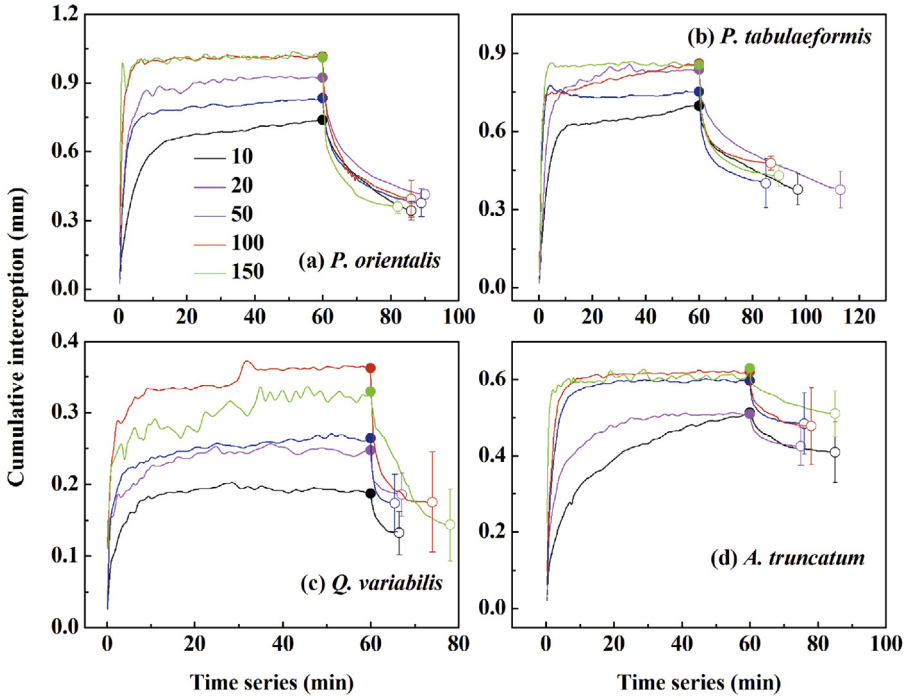

Fig. 2. Time series of average accumulative interception storage per crown projected area (CPA) for *P. orientalis* (a), *P. tabulaeformis* (b), *Q. variabilis* (c), and *A. truncatum* (d) at five rainfall intensities. C_{max} and C_{min} are represented by closed and open symbols, respectively. Error bars indicate standard deviation.

Table 2
C_{max} and C_{min} corresponding to each species and rainfall intensity.

Tree species	Rainfall intensity (mm h^{-1})					Mean C_{max} ± STD (mm), mean C_{min} ± STD (mm)
	10	20	50	100	150	
	C_{max} ± STD (mm), C_{min} ± STD (mm)					
PO	0.74 ± 0.07	0.92 ± 0.10	0.83 ± 0.07	1.02 ± 0.14	1.01 ± 0.04	0.88 ± 0.14
	0.34 ± 0.04	0.41 ± 0.02	0.38 ± 0.06	0.39 ± 0.08	0.36 ± 0.03	0.38 ± 0.09
PT	0.70 ± 0.10	0.84 ± 0.08	0.75 ± 0.14	0.86 ± 0.13	0.85 ± 0.14	0.85 ± 0.18
	0.38 ± 0.05	0.38 ± 0.07	0.40 ± 0.09	0.48 ± 0.03	0.43 ± 0.04	0.43 ± 0.10
QV	0.19 ± 0.03	0.25 ± 0.03	0.27 ± 0.11	0.36 ± 0.10	0.33 ± 0.06	0.30 ± 0.10
	0.13 ± 0.02	0.19 ± 0.03	0.17 ± 0.04	0.18 ± 0.07	0.14 ± 0.03	0.17 ± 0.05
AT	0.51 ± 0.11	0.51 ± 0.08	0.59 ± 0.10	0.62 ± 0.11	0.65 ± 0.05	0.59 ± 0.12
	0.41 ± 0.08	0.42 ± 0.05	0.48 ± 0.08	0.48 ± 0.10	0.51 ± 0.06	0.46 ± 0.08

Note: STD = standard deviation.

(±11) across all the species and rainfall intensities, and average C_{min} was 0.38 mm (±0.17) or 1.4% (±1.1%) of gross precipitation. Statistically, mean C_{min} was 60.0% (±14.3%) of mean C_{max}, which indicates that as much as 40.0% of the intercepted rainwater dripped onto the ground. Our experimental results suggest that the wetting, saturation, and drainage phases of interception occur regardless of rainfall intensity.

Due to the difficulty in measuring interception process, it is often simulated in older forests. For instance, Rutter et al. (1971) modeled the interception in a mature forest and found that, for a rainfall intensity of 1.2 mm h^{-1}, interception can be divided into three distinct phases: the wetting phase and drainage phase. When rainfall intensity increased to 12 mm h^{-1}, three phases of interception were found: the wetting phase, the saturation phase, and the drainage phase. Our experimental results suggest that the wetting, saturation, and drainage phases of interception occur regardless of rainfall intensity.

This simulation neglected evaporation for hours after rainfall, which may have overestimated drainage amount as compared outdoor rainfall interception processes. As a result, more continuous and non-destructive mass measurements of intercepted rainwater are needed at a high-time resolution, Methods appropriate for obtaining such measurements include branch-bending (Hancock and Crowther, 1979), gamma-ray-attenuation (Calder and Wright, 1986), strain gauge (Huang et al., 2005), and stem compression (Friesen et al., 2008; van Stan et al., 2011).

Aston (1979) and Pitman (1989) have found that C_{min} can range from 0.03 to 0.46 mm, which is similar to our findings of 0.17 mm (*Q. variabilis*) and 0.46 (*A. truncatum*). Several studies have also determined that 10 to 70% of total intercepted rainwater drains off following rainfall cessation (Rutter et al., 1971; Pitman, 1989; Calder et al., 1996). The variability in these results indicates that the post-rainfall drainage phase deserves further attention. In particular, droplets may coalesce on leaves and branches to form larger drops, and become more erosive to bare soil (Nanko et al., 2011).

We found varying effects of rainfall intensity on C_{max} and C_{min} across the different species. A significant, increasing trend of mean C_{max} and C_{min} with rainfall intensity was only observed for *P. tabulaeformis* (Figs. 3b and 4b, p = 0.047 and 0.006, respectively). For the other three species, the highest C_{max} and C_{min} were not obtained at the highest rainfall intensity of 150 mm h^{-1} (Figs. 3 and 4). This may have occurred because *P. tabulaeformis* had the largest total leaf area and leaf area index of the four sampled species (Table 1). Specifically, the branches occurred in close-proximity to one another,

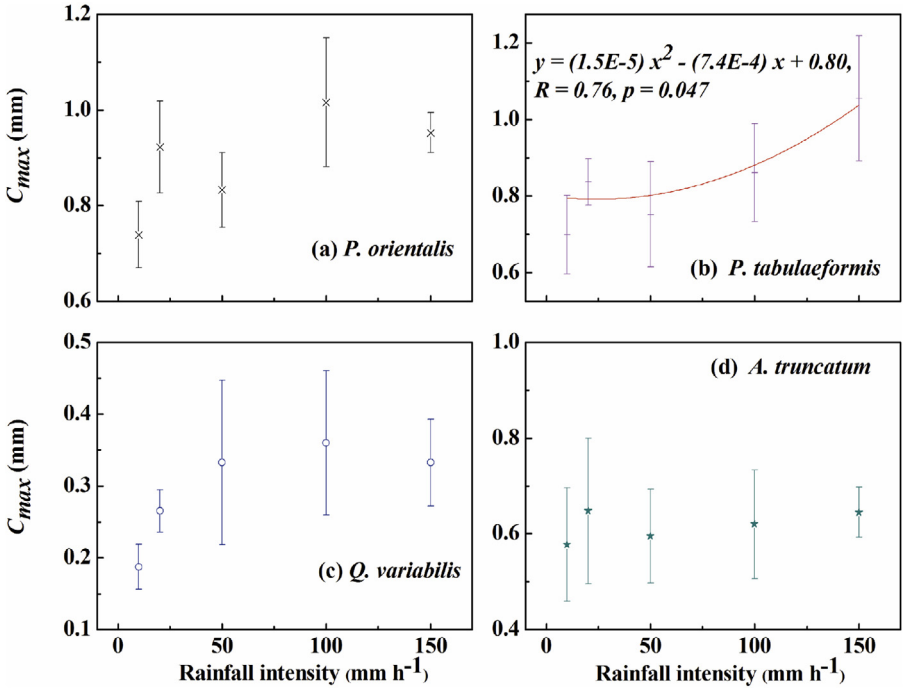

Fig. 3. Relationship between rainfall intensity and average C_{max} for *P. orientalis* (a), *P. tabulaeformis* (b), *Q. variabilis* (c), and *A. truncatum* (d). Error bars indicate standard deviation.

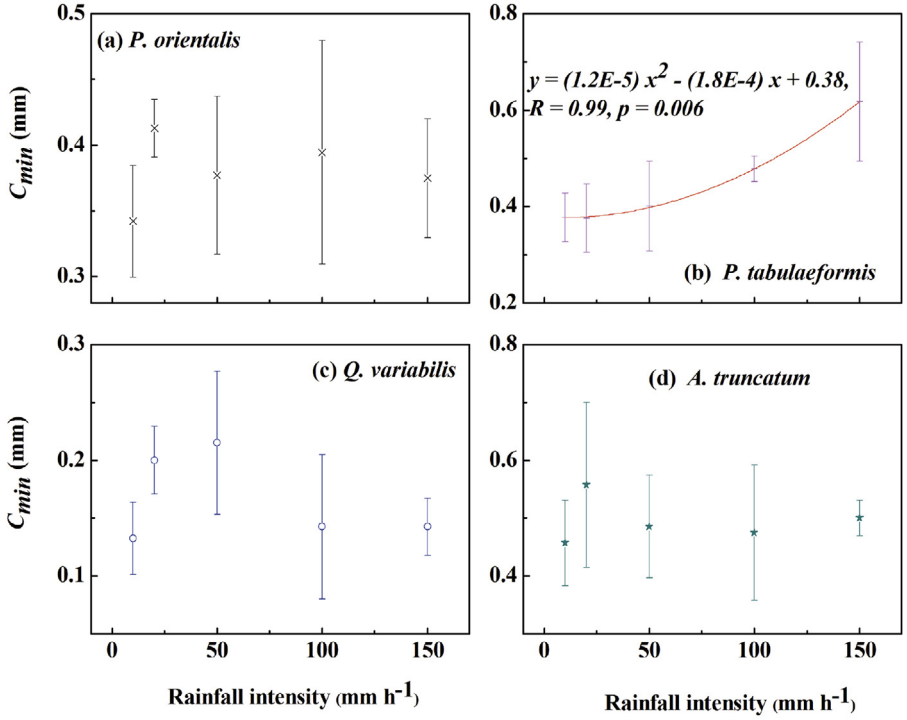

Fig. 4. Relationship between rainfall intensity and average C_{min} for *P. orientalis* (a), *P. tabulaeformis* (b), *Q. variabilis* (c), and *A. truncatum* (d). Error bars indicate standard deviation.

causing a 'multi-layer interception' effect in which rainwater was intercepted by the upper layer of the crown and subsequently was re-intercepted by the lower layer. Hence, branches and needles were gradually wetted, resulting in partially cohered and overlapping branches, particularly at high rainfall intensities (100 and 150 mm h^{-1}).

Previous studies have also reported different trends of C_{max} and C_{min} with increasing *RI*. Wang et al. (2007) reported that a decrease of 0.12 mm in interception as rainfall intensity increased from 33.6 mm h^{-1} to 125.4 mm h^{-1} for a 4.8 m tall *Acer mono* tree. While other studies have shown that C_{max} can increase by 0.07 to 0.2 mm with incremental increases in rainfall intensity (Aston, 1979; Keim et al., 2006). However, a 98 mm h^{-1} rainfall intensity used in one study was relatively high for the small trees (1.3–1.7 m tree height), which may quickly dampen and also seriously shake off retaining drops from the crown (Aston, 1979). Meanwhile, Keim et al. (2006) merely examined the rainfall intensity-C_{max} response for single branches from different positions of the crown (upper, middle, and lower). The response they found may not be applicable to lower branches because these branches mainly receive drips that are possibly larger in size from upper branches in the crown.

Conflicting relationships between C_{min} and rainfall intensity have been reported. Some research has shown C_{min} to decrease with increasing rainfall intensity (Calder, 1996; Price and Carlyle-Moses, 2003), while others have found that C_{min} increased with increasing rainfall intensity (Klaassen et al., 1998; Peng et al., 2014). In our study, small and large rainfall intensities showed different interaction mechanisms with foliage and branch surfaces (also see Bassette and Bussière, 2008). For small rainfall intensities (<30 mm h^{-1}), no splash was observed when raindrops hit the branch and leaf surfaces because the relatively small median raindrop diameters and kinetic energy allowed the intercepted water to cumulate on the branches and leaves. While the opposite pattern occurred for large *RI*s (100 and 150 mm h^{-1}): raindrop splash occurred when energetic raindrops struck and shook the crown. Therefore, the split droplets could have been temporarily intercepted but tended to fall off from leaf surfaces under the repeated agitation, which is likely why fluctuations in cumulative interception at rainfall intensity of 150 mm h^{-1} were observed (Fig. 2). This alternate rainfall intensity–interception mechanism should be further tested at a wide range of rainfall intensities.

Both the ratios of C_{max} and C_{min} as a percentage of gross precipitation (P_g) were significantly correlated ($R > 0.8$, $p < 0.05$) with P_g as a power-decreasing trend (Fig. 5); mean C_{max}/P_g percentage decreased from 5.5% to 0.5% when P_g increased from 10 to 150 mm, while C_{min}/P_g percentage decreased from 3.2% to 0.3% over the same

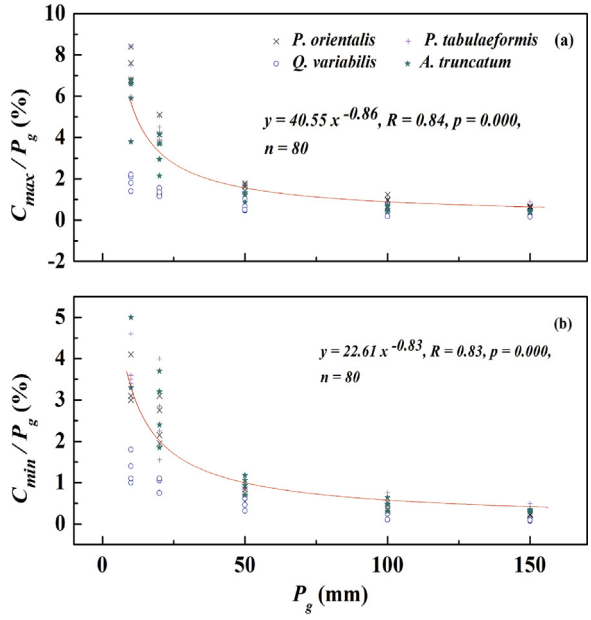

Fig. 5. Variation trend of proportion of C_{max} (a) and C_{min} (b) in gross precipitation (P_g) with increasing precipitation gross (P_g) for all the four species. $n = 80$.

P_g range. Similarly, previous studies reported that interception as a percentage of gross precipitation decreased from 100% to 4% as P_g increased from 1 mm to 50 mm (Crockford and Richardson, 1990a; Staelens et al., 2008; David et al., 2006; Livesley et al., 2014; Peng et al., 2014; Sadeghi et al., 2015).

3.2. Effect of crown traits on rainfall interception

The cumulative interception storage, C_{max}, and C_{min} varied with tree species (Fig. 2). Mean cumulative interception at the 1st and 10th minute was 2.0 and 2.1 times larger for the needle species than the broadleaf species, regardless of rainfall intensity. Significant differences in C_{max} were found between the needle and broadleaf species ($p < 0.05$). The greatest C_{max} was obtained from *P. orientalis* and *P. tabulaeformis*, which was on average 1.9 times greater than that of the broadleaf species. This phenomenon likely results from the fundamental differences in crown structure. The needle species had the largest mean LAI (2.33 for *P. orientalis* and 3.33 for *P. tabulaeformis*) compared with *Q. variabilis* (mean LAI = 1.81) and *A. truncatum* (mean LAI = 1.47), revealing that they had a tighter crown shape than the broadleaf species. Moreover, the needle species had denser and more overlapping branches and foliage than broadleaf species. The minimum leaf density for *P. orientalis* and *P. tabulaeformis* was approximately 23,742 and 9766, which were much larger than those of *Q. variabilis* (296) and *A. truncatum* (247) (Table 1). The larger minimum leaf density for the coniferous species likely increased the contact frequency between foliage and raindrops. Additionally, the mean distance between needles was 0.11 and 0.12 cm for *P. orientalis* and *P. tabulaeformis*, versus 1.45 and 6.32 cm for *Q. variabilis* and *A. truncatum*. A larger minimum leaf density combined with smaller mean distance between needles would suggest that the needles cohered easily to form several fascicles, which could hold water during rainfall events. In contrast, broadleaf species stored less water due to their relatively open crowns, small minimum leaf densities, large mean distance between leaves, steep leaf angle (especially under large rainfall intensities), and probable hydrophobicity caused by glabrous juvenile leaves (Crockford and Richardson, 1990b; Holder, 2013). Some studies have suggested doubling the leaf area of broadleaf species when estimating interception since the other side of leaf can intercept splash droplets as well (Herwitz, 1985). However, the underside of most of the broad leaves in our study remained relatively dry after rainfall.

After rainfall cessation, nearly 49.7% of C_{max} drained off in needle species within 31 min after rainfall. In contrast, this drainage phase lasted only 15 min for broadleaf species with 31.3% of C_{max} draining off of the foliage. *A. truncatum* had the largest C_{min} for all rainfall intensities. Previous studies have found that C_{min} in needle-species is larger than broadleaf species. Barbier et al. (2009) reviewed 28 world-wide interception experiments and found that C_{min} in evergreen conifers was 1.2 times greater than deciduous broadleaves. Similar results have been found for saplings and branches (Aston, 1979; Keim et al., 2006). Our results were slighted different from those reported values because the uneven surfaces of the broadleaf species used in our study had curled margins, clear veins, and pits that likely inhibited the movement of small water droplets. As a result, these small droplets failed to coalesce into larger ones that would have promoted more drainage. Additionally, the branch surface of *A. truncatum* contained concave fissures, which may store more rainwater than the smooth branch surfaces of the needle species. This effect was not detectable during rainfall since the branch and stem flow velocity were larger than post-rainfall velocity. For needle species, a large proportion of intercepted water dripped off after rainfall, which is probably because the clustered branches and needles eventually detached with the continual drip.

Table 3
Pearson's rank correlation coefficients between C_{max} (and C_{min}) and tree structure metrics.

Parameter	C_{max} (mm)	C_{min} (mm)
Height (H, m)	−0.44***	−0.25*
Crown height (CH, m)	−0.47***	−0.28*
Basal diameter(D_B, cm)	−0.16	0.03
Leaf area index (LAI)	0.48***	0.29**
Crown projected area (CPA, m^2)	−0.03	0.27*
Total leaf area (TLA, m^2)	0.34***	0.46***
Woody surface area (WSA, m^2)	0.24*	0.58***
Total surface area (TSA, m^2)	0.36***	0.53***
Mean primary branch angle (MPBA,°)	0.28**	0.23*
Leaf biomass (LB, kg)	0.65***	0.31**
Woody biomass (WB, kg)	0.49***	0.67***
Total biomass (TB, kg)	0.65***	0.57***
Total leaf count (TLC, n)	0.64***	0.21
Total branch count (TBC, n)	0.18	0.48***
Minimum leaf density (LD_{min}, $n\,m^{-3}$)	0.59***	0.20
Minimum branch density (BD_{min}, $n\,m^{-3}$)	0.50***	0.39***
Mean leaf count per branch (MLC, n)	0.65***	0.30**
Total branch length (TBL, m)	0.32**	0.52***

Note: (1) 2-tailed test of significance is used. (2) Significant correlations ($p < 0.05$) are labeled in asterisks: * $p < 0.05$; ** $p < 0.01$; *** $p < 0.001$.

It is reasonable that *Q. variabilis*, which had the lowest total leaf area, total surface area, total biomass, total branch count, and total branch length, generated the lowest C_{max} and C_{min}.

Pearson's correlation analysis showed that both C_{max} and C_{min} were significantly related ($p < 0.05$) to a number of tree structure metrics (Table 3). In particular, biomass (i.e., woody biomass, total biomass), surface area (i.e., total leaf area, total surface area), and branch traits (i.e., minimum branch density) showed the strongest correlations ($p < 0.001$) with C_{max} and C_{min}. In addition, biomass metrics (i.e., leaf biomass, total biomass), and mean leaf count per branch best captured the linear increasing trend with C_{max} ($R = 0.65$). A high leaf biomass and number of leaves per branch can decrease crown openness and gap size, thus increasing the amount of water intercepted during rainfall. Woody biomass was also significantly correlated with C_{min} ($R = 0.67$). Therefore, we found that the best predictors of interception across species were biomass-related parameters. In contrast, Keim et al. (2006) found that leaf and branch biomass was not well correlated with C_{max}, although their study contained a limited number of single branches (51). These conflicting results suggest that additional studies are needed to examine the biomass-interception relations for entire crowns.

Studies have reported that leaf area metrics (i.e., total leaf area, leaf area index, and total surface area) were significantly correlated ($p < 0.05$) with interception (Pitman, 1989; Gómez et al., 2001; Fleischbein et al., 2005; Galdosa et al., 2012), our study showed similar results with R ranging from 0.29 to 0.53. We also found that, in addition to leaf characteristics, branch traits may significantly affect C_{max} and C_{min}. This may be due to the funnel-like crown architecture and branch properties of trees used in our study, as the branch angles in the upper crown were mostly less than 45°, thereby directing water flow along the branch to the trunk instead of draining off. Additionally, the branch surfaces in our study showed great potential to intercept rainfall: the maximum water storage capacity of woody surfaces (S_W) was on average 2.6 times larger than leaves (S_L) (Table 4). This is in accordance with previous studies (Herwitz, 1985; Liu, 1998; Staelens et al., 2006) and suggests that branches may have played a larger role in interception after the leaves were completely wetted during rainfall. Furthermore, the role that branches play in the interception process may be larger for mature trees, since branch surfaces become more fissured and rough with age, which will enable more absorption.

Table 4
Maximum water storage capacity for leaf, branch and stem, and the whole tree.

Tree species	Mean $S_L \pm$STD (mm)	Mean $S_W \pm$STD (mm)	Mean $S \pm$STD (mm)
P. orientalis	0.28 ± 0.06	0.82 ± 0.10	1.10 ± 0.13
P.tabulaeformis	0.22 ± 0.05	0.78 ± 0.11	1.00 ± 0.16
Q. variabilis	0.24 ± 0.04	0.62 ± 0.04	0.86 ± 0.03
A. truncatum	0.33 ± 0.03	0.90 ± 0.11	1.23 ± 0.08

4. Conclusions

This research addressed two major issues of crown interception: process-based rainfall interception characterization, and its response to varying rainfall and crown structure traits. Interception is a dynamic process with three distinct phases regardless of species or rainfall intensity: a wetting phase, a saturation phase, and a post-rainfall drainage phase. Despite the distinct phases, C_{max} and C_{min} varied with species and rainfall intensity. A series of leaf and branch traits including branch count, length, and density were significantly correlated with C_{max} and C_{min}, and the best predictors for interception were biomass-related parameters (i.e., woody biomass and total biomass). The broadleaf species *A. truncatum* had the largest C_{min} when compared with the two needle species of the same age. Consequently, this work has enhanced our understanding of the entire rainfall interception process and its controlling factors. In addition to leaf parameters, branch and biomass related metrics should be included in future hydrological models to better simulate interception and calculate water budgets.

Acknowledgements

We thank the Jiu Feng National Forest Park Administration, postgraduates Jun Xu, Chen Meng, and Pengwei Bao for their help and support in the experiment. We also thank the two anonymous reviewers for their thoughtful recommendations which have greatly improved the manuscript. This study was supported by the Chinese Scholarship Council Fund; Fundamental Research Funds for the Central Universities (no. TD2011-03, no. BLYJ201406); National Natural Science Foundation of China (41171028); Central Nonprofit Research Institutions Basic Scientific Research Special Fund (HKY-JBYW-2016-04); Key Laboratory of the Loess Plateau Soil Erosion and Water Loss Process and Control of Ministry of Water Resources Fund (2015004). None of the funders had any involvement in study design, data collection and analysis, preparation of the manuscript, nor the decision to submit and publish.

References

Aston, A.R., 1979. Rainfall interception by eight small trees. J. Hydrol. 42, 383–396, http://dx.doi.org/10.1016/0022-1694(79)90057-X.
Barbier, S., Balandier, P., Gosselin, F., 2009. Influence of several tree traits on rainfall partitioning in temperate and boreal forests: a review. Ann. For. Sci. 66, 602–612, http://dx.doi.org/10.1051/Forest/2009041.
Bassette, C., Bussière, F., 2008. Partitioning of splash and storage during raindrop impacts on banana leaves. Agric. For. Meteorol. 148, 991–1004, http://dx.doi.org/10.1016/j.agrformet.2008.01.016.
Calder, I.R., 1996. Dependence of rainfall interception on drop size: 1. Development of the two-layer stochastic model. J. Hydrol. 185, 363–378, http://dx.doi.org/10.1016/0022-1694(95)02998-2.
Calder, I.R., Hall, R.L., Rosier, P.T.W., Bastable, H.G., Prasanna, K.T., 1996. Dependence of rainfall interception on drop size: 2. Experimental determination of the wetting functions and two-layer stochastic model parameters for five tropical tree species. J. Hydrol. 185, 379–388, http://dx.doi.org/10.1016/0022-1694(95)02999-0.
Calder, I.R., Wright, I.R., 1986. Gamma ray attenuation studies of interception from Sitka spruce; some evidence for an additional transport mechanism. Water Resour. Res. 22, 409–417, http://dx.doi.org/10.1029/WR022i003p00409.
Carlyle-Moses, D.E., Gash, J.H.C., 2011. Rainfall interception loss by foest canopies. In: Levia, D.F., Carlyle-Moses, D.E., Tanaka, T. (Eds.), Forestry Hydrology and Biogeochemistry: Synthesis of Past Research and Future Directions. Springer Inc, Dordrecht, pp. 407–423.
Chen, D., Yu, X., Liao, B., 2005. Analysis on the function of water conservation of the Chinese forest ecosystem. World For. Res. 18, 49–54 (In Chinese with English Abstract).
Crockford, R.H., Richardson, D.P., 1990a. Partitioning of rainfall in a eucalypt forest and pine plantation in southeastern Australia: III. Determination of the canopy storage capacity of a dry sclerophyll eucalypt forest. Hydrol. Process. 4, 157–167, http://dx.doi.org/10.1002/hyp.3360040206.
Crockford, R.H., Richardson, D.P., 1990b. Partitioning of rainfall in a eucalypt forest and pine plantation in Southeastern Australia: IV. The relationship of interception and canopy storage capacity, the interception of these forests, and the effect on interception of thinning the pine plantation. Hydrol. Process. 4, 169–188, http://dx.doi.org/10.1002/hyp.3360040207.
David, T.S., Gash, J.H.C., Valente, F., Pereira, J.S., Ferreira, M.I., David, J.S., 2006. Rainfall interception by an isolated evergreen oak tree in a Mediterranean savannah. Hydrol. Process. 20, 2713–2726, http://dx.doi.org/10.1002/hyp.6062.
Diao, J., Lei, X., Hong, L., Rong, J., Shi, Q., 2010. Single leaf area estimation models based on leaf weight of eucalyptus in southern China. J. For. Res. 21, 73–76, http://dx.doi.org/10.1007/s11676-010-0012-4.
Fathizadeh, O., Attarod, P., Keim, R.F., Stein, A., Amiri, G.Z., Darvishsefat, A.A., 2014. Spatial heterogeneity and temporal stability of throughfall under individual Quercus brantii trees. Hydrol. Process. 28, 1124–1136, http://dx.doi.org/10.1002/hyp.9638.
Fleischbein, K., Wilcke, W., Goller, R., Boy, J., Valarezo, C., Zech, W., Knoblich, K., 2005. Rainfall interception in a lower montane forest in Ecuador: effects of canopy properties. Hydrol. Process. 19, 1355–1371, http://dx.doi.org/10.1002/hyp.5562.
Friesen, J., van Beek, C., Selker, J., Savenije, H.H.G., van de Giesen, N., 2008. Tree rainfall interception measured by stem compression. Water Resour. Res. 44, 1–5, http://dx.doi.org/10.1029/2008.wr007074.
Galdosa, F.V., Álvareza, C., Garcíaa, A., Revillaa, J.A., 2012. Estimated distributed rainfall interception using a simple conceptual model and moderate resolution imaging spectroradiometer (MODIS). J. Hydrol. 468, 213–228, http://dx.doi.org/10.1016/j.jhydrol.2012.08.043.
Gerrits, A.M.J., Pfister, L., Savenije, H.H.G., 2010. Spatial and temporal variability of canopy and forest floor interception in a beech forest. Hydrol. Process. 24, 3011–3025, doi: 10 1002/hy p.7712.
Gerrits, A.M.J., Savenije, H.H.G., 2011. Treatise on Water Science. Elsevier, Oxford.
Gómez, J.A., Giráldez, J.V., Fereres, E., 2001. Rainfall interception by olive trees in relation to leaf area. Agric. Water Manage. 49, 65–76, http://dx.doi.org/10.1016/S0378-3774(00)00116-5.
Guevara-Escobar, A., González-Sosa, E., Véliz-Chávez, C., Ventura-Ramos, E., Ramos-Salinas, M., 2007. Rainfall interception and distribution patterns of gross precipitation around an isolated Ficus benjamina tree in an urban area. J. Hydrol. 333, 532–541, http://dx.doi.org/10.1016/j.jhydrol.2006.09.017.
Hancock, N.H., Crowther, J.M., 1979. A technique for the direct measurement of water storage on a forest canopy. J. Hydrol. 41, 105–122, http://dx.doi.org/10.1016/0022-1694(79)90109-4.
Herwitz, S.R., 1985. Interception storage capacities of tropical rainforest canopy trees. J. Hydrol. 77, 237–252, http://dx.doi.org/10.1016/0022-1694(85)90209-4.
Holder, C.D., 2013. Effects of leaf hydrophobicity and water droplet retention on canopy storage capacity. Ecohydrology 6, 483–490, http://dx.doi.org/10.1002/eco.1278.
Horton, B.E., 1919. Rainfall interception. Mon. Weather Rev. 47, 603–623.
Huang, Y.S., Chen, S.S., Lin, T.P., 2005. Continuous monitoring of water loading of trees and canopy rainfall interception using the strain gauge method. J. Hydrol. 311, 1–7, http://dx.doi.org/10.1016/j.jhydrol.2004.08.036.
Huo, Y., Bi, H., Zhu, Y., Xu, H., Wang, X., Chang, Y., 2015. Characteristics of artificial rainfall produced by QYJY-503 C simulation system. Sci. Soil Water Conserv. 2, 31–36 (In Chinese with English Abstract).
Keim, R.F., Skaugset, A.E., Weiler, M., 2006. Storage of water on vegetation under simulated rainfall of varying intensity. Adv. Water Resour. 29, 974–986, http://dx.doi.org/10.1016/j.advwatres.2005.07.017.
Klaassen, W., Bosveld, F., Water, E.D., 1998. Water storage and evaporation as constituents of rainfall interception. J. Hydrol. 212-213, 36–50, http://dx.doi.org/10.1016/S0022-1694(98)00200-5.
Kimmins, J.P., 1973. Some statistical aspects of sampling throughfall precipitation in nutrient cycling studies in British Columbian coastal forests. Ecology 54, 1008–1019.
Kobayashi, H., Ryu, Y., Baldocchi, D.B., Welles, J.M., Norman, J.M., 2013. On the correct estimation of gap fraction: how to remove scattered radiation in gap fraction measurements? Agric. For. Meteorol. 174-175, 170-183, http://dx.doi.org/10.1016/j.agrformet.2013.02.013.
Levia, D.F., Michalzik, B., Näthe, K., Bischoff, S., Richter, S., Legates, D.R., 2015. Differential. stemflow yield from European beech saplings: the role of individual canopy structure metrics. Hydrol. Process. 29, 43–51, http://dx.doi.org/10.1002/hyp.10124.
Li, X., Niu, J., Xie, B., 2013. Study on hydrological functions of litter layers in North China. PLoS ONE 8, 1–13, http://dx.doi.org/10.1371/journal.pone.0070328.
Liu, S.G., 1998. Estimation of rainfall storage capacity in the canopies of cypress wetlands and slash pine uplands in North-Central Florida. J. Hydrol. 207, 32–41, http://dx.doi.org/10.1016/S0022-1694(98)00115-2.
Livesley, S.J., Baudinette, B., Glover, D., 2014. Rainfall interception and stem flow by eucalypt street trees—the impacts of canopy density and bark type. Urban For. Urban Green 13, 192–197, http://dx.doi.org/10.1016/j.ufug.2013.09.001.

Llorens, P., Domingo, F., 2007. Rainfall partitioning by vegetation under Mediterranean conditions. A review of studies in Europe. J. Hydrol. 335, 37–54, http://dx.doi.org/10.1016/j.jhydrol.2006.10.032.
Ministry of Water Resources of P.R. China, 2013. Bulletin of First National Water Census for Soil and Water Conservation., pp. 1–8, ⟨http://202.96.31.90/pic/article/GovFile/articlegov/2013/07/11/2968126/C76B97321AFA3F222FB237C1021AFC3A.pdf⟩ [Online] (In Chinese).
Ministry of Water Resources of P.R China, 2011. China Water Resources Bulletin. China Water & Power Press, Beijing, pp. 51.
Morgan, R.P.C., 2005. Soil erosion and conservation. Blackwell Publishing, Malden, pp. 304.
Murray, S.J., 2014. Trends in 20th century global rainfall interception as simulated by a dynamic global vegetation model: implications for global water resources. Ecohydrology 7, 102–114, http://dx.doi.org/10.1002/eco.1325.
Muzylo, A., Llorens, P., Valente, F., Keizer, J.J., Domingo, F., Gash, J.H.C., 2009. A review of rainfall interception modelling. J. Hydrol. 370, 191–206, http://dx.doi.org/10.1016/j.jhydrol.2009.02.058.
Nanko, K., Onda, Y., Ito, A., Moriwaki, H., 2011. Spatial variability of throughfall under a single tree: experimental study of rainfall amount, raindrops, and kinetic energy. Agric For. Meteorol. 151, 1173–1182, http://dx.doi.org/10.1016/j.agrformet.2011.04.006.
Nanko, K., Watanabeb, A., Hottac, N., Suzuki, M., 2013. Physical interpretation of the difference in drop size distributions of leaf drips among tree species. Agric For. Meteorol. 169, 74–84, http://dx.doi.org/10.1016/j.agrformet.2012.09.018.
Peng, H., Zhao, C., Feng, Z., Xu, Z., Wang, C., Zhao, Y., 2014. Canopy interception by a spruce forest in the upper reach of Heihe River basin, Northwestern China. Hydrol. Process. 28, 1734–1741, http://dx.doi.org/10.1002/hyp.9713.
Pitman, J.I., 1989. Rainfall interception by Bracjen in open habitats—relations between leaf area, canopy storage and drainage rate. J. Hydrol. 105, 317–334, http://dx.doi.org/10.1016/0022-1694(89)90111-X.
Price, A.G., Carlyle-Moses, D.E., 2003. Measurement and modelling of growing-season canopy water fluxes in a mature mixed deciduous forest stand, southern Ontario, Canada. Agric For. Meteorol. 119, 69–85, http://dx.doi.org/10.1016/s0168-1923(03)00117-5.
Rutter, A.J., Kershaw, K.A., Robins, P.C., Morton, A.J., 1971. A predictive model of rainfall interception in forests, 1. Derivation of the model from observations in a plantation of Corsican pine. Agric. Meteorol. 9, 367–384, http://dx.doi.org/10.1016/0002-1571(71)90034-3.
Sadeghi, S.M.S., Attarod, P., Van Stan, J.T., Pypker, T.G., Dunkerley, D., 2015. Efficiency of the reformulated Gash's interception model in semiarid afforestations. Agric For. Meteorol. 201, 76–85, http://dx.doi.org/10.1016/j.agrformet.2014.10.006.
Sutanto, S.J., Wenninger, J., Coenders-Gerrits, A.M.J., Uhlenbrook, S., 2012. Partitioning of evaporation into transpiration, soil evaporation and interception: a comparison between isotope measurements and a HYDRUS-1D model. Hydrol. Earth Syst. Sci. 16, 2605–2616, http://dx.doi.org/10.5194/hess-16-2605-2012.
Savenije, H.H.G., 2004. The importance of interception and why we should delete the term evapotranspiration from our vocabulary. Hydrol. Process. 18, 1507–1511, http://dx.doi.org/10.1002/hyp.5563.
Staelens, J., De Schrijver, A., Verheyen, K., Verhoest, N.E.C., 2006. Spatial variability and temporal stability of throughfall water under a dominant beech (*Fagus sylvatica* L.) tree in relationship to canopy cover. J. Hydrol. 330, 651–662, http://dx.doi.org/10.1016/j.jhydrol.2006.04.032.
Staelens, J., De Schrijver, A., Verheyen, K., Verhoest, N.E.C., 2008. Rainfall partitioning into throughfall, stemflow, and interception within a single beech (*Fagus sylvatica* L.) canopy: influence of foliation, rain event characteristics, and meteorology. Hydrol. Process. 22, 33–45, http://dx.doi.org/10.1002/hyp.6610.
van Dijk, A.I.J.M., Gash, J.H., van Gorsel, E., Blanken, P.D., Cescatti, A., Emmel, C., Gielen, B., Harman, I.N., Kiely, G., Merbold, L., Montagnani, L., Moors, E., Sottocornola, M., Varlagin, A., Williams, C.A., Wohlfahrt, G., 2015. Rainfall interception and the coupled surface water and energy balance. Agric. For. Meteorol 214–215, 402–415, http://dx.doi.org/10.1016/j.agrformet.2015.09.006.
van Stan, J.T., Jarvis, M.T., Levia, D.F., Friesen, J., 2011. Instrumental method for reducing error in compression-derived measurements of rainfall interception for individual trees. Hydrol. Sci. J 56, 1061–1066, http://dx.doi.org/10.1080/02626667.2011.590811.
Wang, A., Diao, Y., Pei, T., Jin, C., Zhu, J., 2007. A semi-theoretical model of canopy rainfall interception for a broad-leaved tree. Hydrol. Process. 21, 2458–2463, http://dx.doi.org/10.1002/hyp.6413.
Wang, S., Fu, B.J., He, C.S., Gao, G.Y., 2011. A comparative analysis of forest cover and catchment water yield relationships in northern China. For. Ecol. Manage. 262, 1189–1198, http://dx.doi.org/10.1016/j.foreco.2011.06.013.
Wang, J., Shang, Y., Wang, H., Zhao, Y., Yin, Y., 2015. Beijing's water resources: challenges and solutions. J. Am. Water Resour. Assoc. 51, 614–623, http://dx.doi.org/10.1111/1752-1688.12315.
Xiao, Q.F., McPherson, E.G., 2015. Surface water storage capacity of twenty tree species in Davis, California. J. Environ. Qual. 44, 291–302, http://dx.doi.org/10.2134/jeq2015.02.0092.
Xiao, Q.F., McPherson, E.G., 2011. Rainfall interception of three trees in Oakland, California. Urban Ecosyst. 14, 755–769, http://dx.doi.org/10.1007/s11252-011-0192-5.
Xiao, Q.F., McPherson, E.G., Ustin, S.L., Grismer, M.E., Simpson, J.R., 2000a. Winter rainfall interception by two mature open-grown trees in Davis, California. Hydrol. Process. 14, 763–784, http://dx.doi.org/10.1002/(Sici)1099-1085(200003)14:4<763::Aid-Hyp971>3.3.Co;2-Z.
Xiao, Q.F., McPherson, E.G., Ustin, S.L., Grismer, M.E., 2000b. A new approach to modeling tree rainfall interception. J. Geophys. Res. 105, 29173–29188, http://dx.doi.org/10.1029/2000jd900343.
Xiao, Q.F., McPherson, E.G., 2003. Rainfall interception by Santa Monica's municipal urban forest. Urban Ecosyst. 6, 291–302, http://dx.doi.org/10.1023/B:UECO.0000004828.05143.67.
Zhong, Y.D., Jia, Y.W., Li, Z.W., 2013. Spatial and temporal changes of maximum 1 h precipitation intensity in Beijing region in last 53 years. J. Chin. Hydrol. 33, 32–37 (In Chinese with English Abstract).